International Soil and Water Conservation Research ▮ (▮▮▮▮) ▮▮▮–▮▮▮

HOSTED BY

Contents lists available at ScienceDirect

International Soil and Water Conservation Research

journal homepage: www.elsevier.com/locate/iswcr

Original Research Article

Estimating soil erosion response to land use/cover change in a catchment of the Loess Plateau, China

Rui Yan [a], Xiaoping Zhang [a,*], Shengjun Yan [b], Hao Chen [a]

[a] State Key Laboratory of Soil Erosion and Dry land Farming on the Loess Plateau, Northwest A & F University; Institute of Soil and Water Conservation, Chinese Academy of Sciences and Ministry of Water Resources, Yangling, Shaanxi 712100, China

[b] State Key Laboratory of Water Environment Simulation, School of Environment, Beijing Normal University, Beijing 100875, China

ARTICLE INFO

Article history:
Received 4 March 2017
Received in revised form
2 November 2017
Accepted 13 December 2017

Keywords:
Loess Plateau
Land use changes
RUSLE
SEDD
Soil erosion

ABSTRACT

The vegetation restoration project, named the Grain to Green Program, has been operating for more than ten years in the upper reaches of the Beiluo River basin, located in the Loess Plateau of China. It is significant to be able to estimate the success of preventing soil erosion. In this study, the Revised Universal Soil Loss Equation (RUSLE) and the Sediment Distributed Delivery (SEDD) model were used to assess the annual soil loss derived from water erosion. The results showed that the study area suffered from primary land use changes, with increasing grassland and forest and decreasing farmland from 1990 to 2010. Based on that, the average soil erosion modulus decreased from 18,189.72 t/(km^2 a) in 1990–7408.93 t/(km^2 a) in 2000 and 2857.76 t/(km^2 a) in 2010. Compared with 1990, the average soil erosion modulus decreased by 59.0% and 84.3% for 2000 and 2010, respectively. Benefiting from the increased vegetation coverage and improved ecological environment, the soil erosion in this study area clearly declined. This research also found that the distribution of the three years of soil erosion was similarly based on topographic factors. The soil erosion modulus varied with different land use types and decreased in the order of residential area > farmland > grassland > forest. The average soil erosion modulus gradually increased with the increase of the slope gradient, and 76.08% of the total soil erosion was concentrated in the region with a gradient more than 15 degrees. The soil erosion modulus also varied with slope aspects in the order of sunny slope > half-sunny slope > half-shady slope > shady slope. This research provides useful reference for soil and water conservation and utilization in this area and offers a technical basis for using the RUSLE to estimate soil erosion in the Loess Plateau of China.

1. Introduction

Soil erosion, a widespread form of soil degradation, is one of the most severe threats to the terrestrial ecosystems in the world (Pimental, Harvey, & Resosudarmo, 1995). It is directly related to decreased agriculture productivity and water pollution, and it has many negative effects on nature, such as degradation of soil structure, depletion of soil fertility, reducing the effective rooting depth, and ruining the most fundamental of all natural resources (Fitton, Saffouri, & Blair, 1995; Lal & Bruce, 1999; Nearing, 2005).

The Chinese Loess Plateau is the most heavily eroded area in the world (Fu, 1989), and the soil erosion modulus with 5000–10,000 mg km^{-2} per year were larger than other areas (Chen, Wang, Fu, & Qiu, 2001). Since the 1950s, to control severe soil erosion, improve agriculture production and reduce sediment loads in the Yellow River, there has been implemented a lot of soil and water conservation projects in the Loess Plateau catchments. In order to promote sustainable development in the Loess Plateau, the Grain for Green project was implemented in 1999. These conservation efforts, including terracing, afforestation and vegetation restoration, reduced the sediment yield from hill slopes and sediment delivery to rivers by increasing hydrologic surface roughness, and the vegetation coverage gradually increased (Chen, Ma, & Zhang, 2016; Yan, Zhang, Yan, & Zhao, 2016). Generally, the more the vegetation restoration implemented in the region, and the lower the soil erosion modulus (Ritsema, 2003).

Soil erosion caused by water has been assessed by some developed models, including the Water Erosion Prediction Project (WEPP), Universal Soil Loss Equation (USLE), the Revised Universal Soil Loss Equation (RUSLE), and the Erosion Productivity Impact Calculator (EPIC) (Flanagan & Laflen, 1997; Renard, Foster, & Weesies, 1997; Williams, Renard, & Dyke, 1983; Wischmeier & Smith, 1978). The USLE model considers most of the factors to assess long term soil erosion from interrill and rill areas

* Corresponding author.
E-mail address: zhangxp@ms.iswc.ac.cn (X. Zhang).

https://doi.org/10.1016/j.iswcr.2017.12.002

(Wischmeier & Smith, 1978). Compared to the USLE, the RUSLE has become available during the last 40 years with the characteristics of easily to parameterize and requiring less data (Lee, 2004). The combination of erosion models with GIS was an effective method to assess the temporal and spatial distribution of erosion (Mitasova, Hofierka, Zlocha, & Iverson, 1996; Qin & Zhu, 2009). Ferro and Porto (2000) used the USLE combined with the travel time concept and assessed the erosion in a watershed.

There have many researches to investigate soil erosion either in plot or watershed scale in the Loess Plateau of China (Fu, Wang, & Lu, 2009; Sun, Shao, & Liu, 2013; Zhao, Kondolf, Mu, & Han, 2016). Fu, Zhao, and Chen (2005), based on the RUSLE to assess soil loss in the Yanhe watershed of the Loess Plateau, found that the annual average soil erosion was 14,458 mg km^{-2} per year. Sun, Shao, and Liu (2014) used the RUSLE to analyze the influence of land cover change on soil erosion in the Loess Plateau from 2000 to 2010. The results found that the steadily increased vegetation cover lead to gradually decreased soil erosion rates from 2000 to 2010. Zhao, Kondolf, Mu, and Han (2017) found that the sediment yield also decreased in the Huangfuchuan catchment of the Loess Plateau from 1990 to 2006. A series of previous studies demonstrated that these measures have obtained success to some extent.

The Beiluo River, located in the center of the Loess Plateau, is representative of the changes in vegetation coverage resulting from conservation projects. The mean annual soil erosion modulus in the catchment decreased by 90% under the implementation of projects (Chen et al., 2016). Yan et al. (2016) found that the average annual vegetation coverage in 1990, 2000 and 2010 in the upper reaches of Beiluo River basin were 15.86%, 19.20% and 35.50%, respectively, which showed a gradually increasing trend. Liu et al. (2015) also found that the annual runoff and sediment yield clearly decreased since the implementation of projects. Along with the improved ecological environment, analysis about the temporal and spatial distribution of soil erosion were limited in the upper reaches of the Beiluo River basin. To realize the effect of soil and water conservation on soil erosion and spatial distribution, we selected this basin in the Loess Plateau by combining the RUSLE with the sediment distributed delivery (SEDD) model. In this catchment, the objectives of this study are as follows:

(1) Examine the temporal and spatial variation of soil erosion and sediment yield under the background of land use changes with the SEDD model.
(2) Analyze the impacts of topographic factors including slope gradients and slope aspects on soil erosion in different years.

2. Catchment description and data collection

2.1. Catchment description

The Beiluo River basin (107°33′33″E-110°10′30″E, 34°39′55″N-37°18′22″N) is a secondary tributary of the Yellow River. The upper reaches of the Beiluo River, controlled by the Wuqi gauging station, covers an area of 3408 km^2, which accounts for 12.7% of the Beiluo River basin (Fig. 1). The studied catchment is a typical hilly gully area of the Loess Plateau and has a heavily dissected landscape with gully densities of 6–8 km/km^2. This area is located in a warm temperate semi-arid climate zone, and has clear characteristics of a continental monsoon climate with abundant sunshine and the variation of four seasons. The maximum precipitation was 797.6 mm in 1959, and the minimum precipitation was 320.2 mm in 1995. The mean annual precipitation in the flood season was approximately 391.9 mm and accounted for 76.2% of the annual total precipitation. Temperature gradually decreased from north to south, with part of the study area affected by the characteristics of topography distribution. The soil type in the basin is mainly dominated by loessial soil, dark loessial soil and gray-cinnamon soil. Loess soil is the main soil type of the catchment, and it is the youth directly forming from the Loess parent material, with the characteristics of no obvious profile differentiation. Although it has good permeability, soil erosion, drought and infertility were the prominent problems of Loess soil because of its characteristics, including steep slopes, strong evaporation and weak water

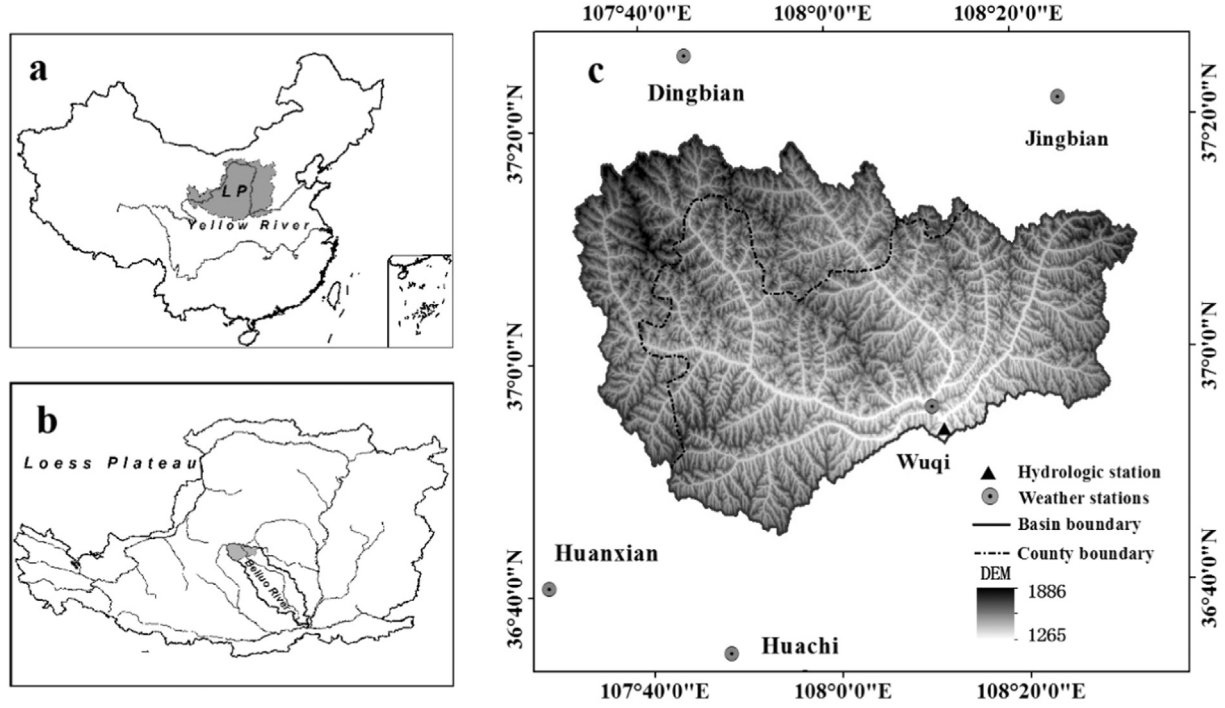

Fig. 1. The locations of the upper reaches of the Beiluo River basin (c) and the LP (Loess Plateau) (b) in China (a). Five weather stations in the studied area (c) were showed as the gray round circle with the dark point inside. The hydrological station showed as dark triangle.

retention.

The featured vegetation is a transitional type from forest to prairie. The natural forest is totally destroyed, and the planted arbors include *Populus simonii, Populus hopeiensis, Robinia pseudoacacia, Prunus armeniaca, Pyrus betulaefolia*, and *Platycladus orientalis*. The small bushes consist of *Hippophae rhamnoides, Caragana korshinskii,* and *Caragana intermedia*. The grass community includes *Salsola collina, Artemisa scoparia, Lespedeza davurica, Artemisa vestita,* and *Bothriochloa ischaemum* (Qin & Zhu, 2009).

3. Methods and datasets

3.1. Datasets

The topography, land use/cover, climate and sediment load data were collected from different sources. Digital elevation model (DEM) data with a 30-m spatial resolution were selected to derive the hydrologic parameters, including slope, flow direction and slope length. Land use maps for 2000 were derived from the National Earth System Science Data Sharing Platform (Loess Plateau Science Data Center, http://loess.data.ac.cn). The land use in 1990 and 2010 were interpreted from Landsat TM images from 1990 and 2010. The dominant land use types included grassland, forest, cropland, residential areas and water. The normalized difference vegetation index (NDVI) data were achieved from the TM imagery data and MODIS data derived from the International Scientific Data Service Platform (http://datamirror.csdb.cn/).

The soil map (1:500,000 scale) was also derived from the National Earth System Science Data Sharing Platform (Loess Plateau Science Data Center). The soil property data related to the soil types in the area were obtained from the Shanxi Soil Database and were used to calculate the K value.

Daily data of precipitation from five meteorological stations within and around the study catchment during 1963–2012 were derived from the information center of the China Meteorological Administration (CMA). Daily sediment load data at the Wuqi station from 1986 to 2012 were selected from the Water Resources Committee of the Yellow River Conservancy Commission. In consistent with the information of land use and land cover, the meteorological data and hydrological data were classified three periods, i.e. 1986–1995, 1996–2006, and 2007–2012, to investigate the spatial temporal trend of soil erosion and sediment load in the catchment. All the spatial data, including land use, DEM, vegetation cover data and soil maps, were resampled using the nearest neighborhood method to the same resolution at the catchment.

3.2. Methods

The SEDD model was established based on the concept of the RUSLE model and was used to estimate the sediment delivery ratios (SDRs) for each catchment unit. The SEDD model was combined with GIS by Jain and Kothyari (2000) in order to process large amounts of spatial data and display the spatial results data. In this study, the gross soil erosion of each grid cell was estimated based on the RUSLE model and the sediment load of each cell was calculated and combined with the SDR of each cell.

3.2.1. Description of the RUSLE model

The annual gross soil erosion (t/ha/a) in each grid cell was calculated as Eq. (1):

$$A_i = R_i K_i L_i S_i C_i P_i \tag{1}$$

where subscript $i = i^{th}$ cell, A_i is the average annual soil loss per each cell (t/ha yr), R_i is the rainfall-runoff erosivity factor (MJ mm/ha h yr), K_i is the soil erodibility factor (t ha h/ha MJ mm), L_i is the slope length factor, S_i is the slope steepness factor, C_i is the cover management factor, and P_i is the conservation support practice factor.

3.2.1.1. Rainfall erosivity factor (R). The rainfall erosivity index (R) is the potential driving force of the rain to cause erosion. Several previous studies have found that it has a direct relationship with soil erosion (Angulo-Martinez & Begueria, 2009; Renard et al., 1997). In this study, the annual rainfall erosivity was calculated according to the method of Zhang and Fu (2003). R was calculated using daily rainfall data based on the accumulation of half-month rainfall erosivity, which was widely used in China (Cheng, Zhao, Zhang, & Xu, 2009; Sun et al., 2013; Xin, Yu, Li, & Lu, 2011; Zhao et al., 2017). The equation used to calculate annual rainfall erosivity is as follows Eqs. (2)–(4).

$$M_i = \alpha \sum_{j=1}^{k} (D_j)^{\beta} \tag{2}$$

$$\beta = 0.8363 + 18.144P_{d12}^{-1} + 24.455P_{y12}^{-1} \tag{3}$$

$$\alpha = 21.586\beta^{7.1891} \tag{4}$$

where M_i is the half-month rainfall erosivity (MJ mm/ha h yr), D_j is the effective rainfall for day j in one half-month (in the standard of China's erosive rainfall, if the actual rainfall for a day is larger than the value of 12 mm, D_j is equal to the actual rainfall; otherwise, D_j is equal to zero), k is the value of the number days in the half-month, P_{d12} is the average daily rainfall that is more than 12 mm, and P_{y12} is the yearly total rainfall for days with rainfall more than 12 mm. The Kriging method was used to interpolate the annual R factor. Mean annual R factor during 2007–2012 was shown in Fig. 2a.

3.2.1.2. Soil erodibility factor (K). The soil erosivity rate (K) represents the susceptibility of soil to erosion (Parysow, Wang, & Gertner, 2003). The K value is different by the parameters of soil texture and organic matter content permeability according to the different soil type (Wischmeier, Johnson, & Cross, 1971). In our study, the K value was calculated by the equation from EPIC as follows Eq. (5) (Williams et al., 1983):

$$\begin{aligned} K = &\left\{0.2 + 0.3exp\left[-0.0256SAN\frac{(1-SIL)}{100}\right]\right\}\left(\frac{SIL}{CLA+SIL}\right)^{0.3} \\ &\times\left(1.0-\frac{0.25C}{C+exp(3.72-2.95C)}\right) \\ &\left(1.0-\frac{0.7SNI}{SNI+exp(-5.51+22.9SNI)}\right)\times 0.1317 \end{aligned} \tag{5}$$

where *CLA*, *SAN* and *SIL* are the fraction (%) of clay, sand and silt, respectively; *C* is the soil organic carbon content (%); and *SNI* is determined by 1-SAN/100. We convert the K value from US customary units to SI units by multiplying by 0.1317. K factor in the catchment was shown in Fig. 2b.

3.2.1.3. Topographic factor (LS). The LS factor reflects the relationship between the slope length and the slope gradient with erosion (Lu, Tenywa, Isabirye, Majaliwa, & Woomer, 2003). Higher slope lengths may increase the overland flow and lead to more soil erosion of the land surface (Zhao et al., 2017). Similarly, higher slope gradients also increase the runoff rate and lead to more soil erosion. Previous research indicates that in the RUSLE model, the

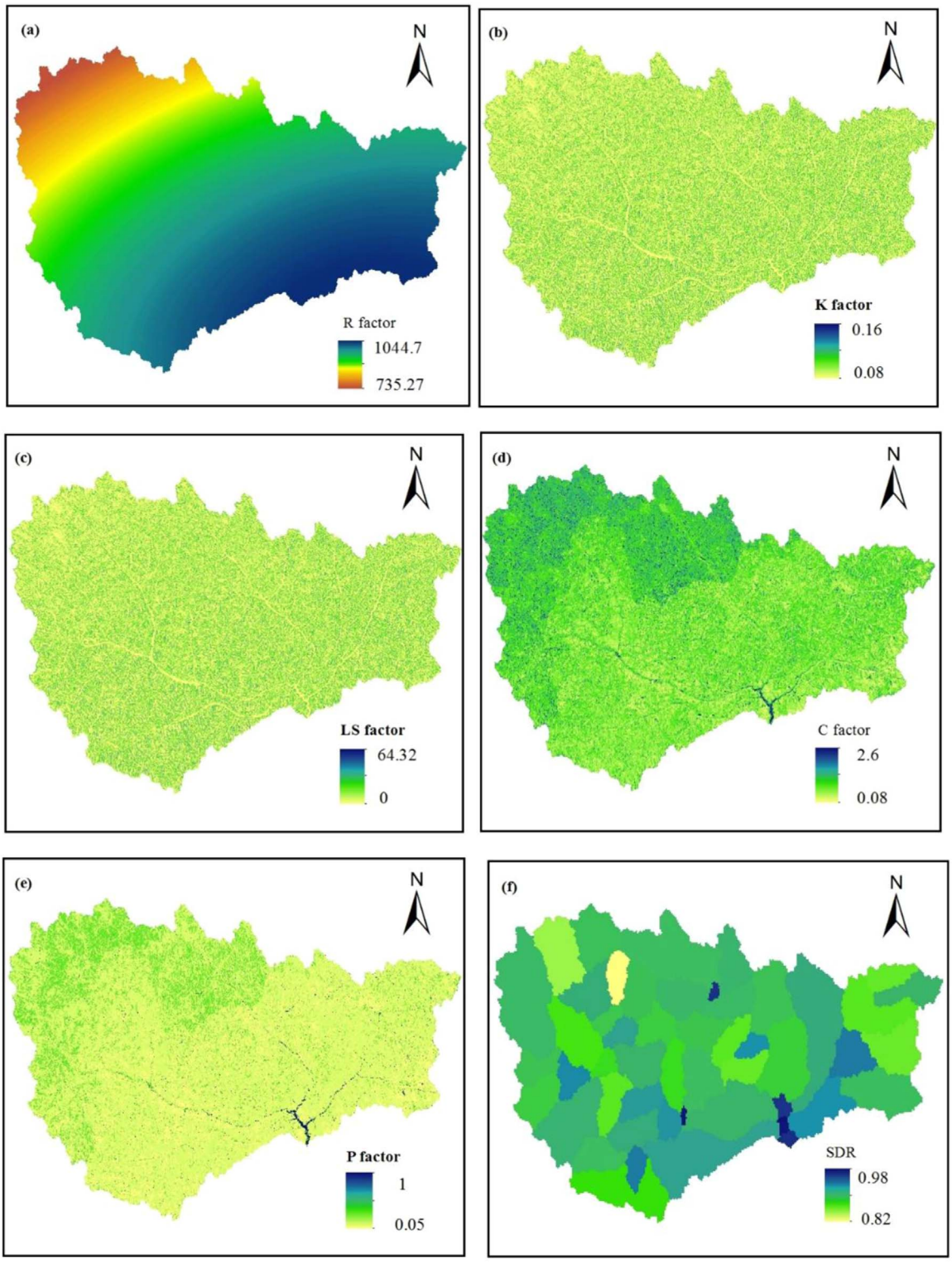

Fig. 2. Soil erosion factors of the RUSLE model in the study area. Mean annual R factor (a) and SDR (f) were for 2007–2012, C (d) and P (e) factors were obtained in the basis of land use and land cover information in 2010.

algorithms of the LS factor was up to slopes $\leq$ 18% because the slopes of the plot data used in the RUSLE only was only up to 18% (McCool, Foster, Mutchler, & Meyer, 1989). In our study area, a small portion of the slopes exceeded 20%. Therefore, in this study, the revised algorithms method within the RUSLE model were selected to calculate the LS factor, which was proposed by Liu, Nearing, and Risse (1994) and Liu, Nearing, Shi, and Jia (2000). The equation is as follows Eqs. (6) and (7):

$$L = \left(\frac{\gamma}{22.13}\right)^{m} \begin{cases} m = 0.5 & \theta \geq 3^{\circ} \\ m = 0.4 & 3^{\circ} > \theta \geq 1.5^{\circ} \\ m = 0.3 & 1.5^{\circ} > \theta \geq 0.5^{\circ} \\ m = 0.2 & 0.5^{\circ} \geq \theta \end{cases} \quad (6)$$

$$S = \begin{cases} 10.8sin\theta + 0.03, & \theta < 9\% \\ 16.8sin\theta - 0.05, & 9\% \le \theta \le 18\% \\ 21.91sin\theta - 0.96, & \theta > 18\% \end{cases} \quad (7)$$

where γ is the slope length (m) and m is determined depending on the percent slope (θ).

The *LS* factor from 30 m DEM in the catchment is shown as Fig. 2c.

3.2.1.4. Vegetation cover factor (C). Renard et al. (1997) indicated that soil loss are most sensitive to the change of vegetation coverage and the relationship between them was negative, but this relationship is limited to the vegetation coverage exceeding 78.3% (Wang & Liu, 1999; Zhang, Liu, Shi, & Jiang, 2001). Cai, Ding, and Shi (2000) calculated the C factor using vegetation coverage data based on the results from many rainfall experimental plots experiments. The equation is expressed as Eq. (8):

$$C = \begin{cases} 1 & f = 0 \\ 0.6508 - 0.3436\log_{10} f & 0 < f \le 78.3\% \\ 0 & f > 78.3\% \end{cases} \quad (8)$$

In this equation, vegetation coverage data was derived from NDVI. Vegetation coverage data was calculated by the equation as follows Eq. (9):

$$f = \frac{(NDVI - NDVI_{soil})}{(NDVI_{max} - NDVI_{soil})} \quad (9)$$

where $NDVI_{max}$ is the *NDVI* value for pixels completely covered by the vegetation and $NDVI_{soil}$ is the *NDVI* value for totally bare soil pixels.

C factor resulted from land use and land cover in 2010 in the catchment is shown as Fig. 2d.

3.2.1.5. Erosion control practice factor (P). P factor presents the effects of practices to reduce the amount of soil erosion. Renard et al. (1997) indicated that it is difficult to determine the P factor, and it was the least reliable factor among the RUSLE input factors. In this study, we used the land use classification map to determine the P factor, referencing the results of Fu et al. (2005) and Sun et al. (2013). In this study, the P values were 0.31, 0.05 and 0.12 for farmland, forest and grassland, respectively, referencing to previous research (Qin & Zhu, 2009; Sun et al., 2013). P factor derived from land use and land cover information in 2010 is shown in Fig. 2e.

3.2.2. Description of the SEDD model

The SEDD model combined with the RUSLE model and the sediment delivery ratio could be used to calculate annual temporal and spatial soil loss and sediment load. The model divided the watershed into sub-watershed units, and Ferro and Minacapilli (1995) proposed that the SEDD model could determine the sediment delivery ratio SDR_i for each grid cell as Eq. (10):

$$SDR_i = exp(-\beta \cdot t_i) = exp\left(-\beta \cdot \sum_{i=1}^{N} \left(\frac{l_i}{v_i}\right)\right) \quad (10)$$

where β is a coefficient related with specific basin; t_i is the travel time from a given cell to the nearest stream cell along the path; N is the total number passes from one cell along the path to the river channel for a cell; l_i is the flow length (m); and v_i is the flow velocity, which can be obtained from the following Eq. (11):

$$v_i = k_i\sqrt{s_i} \quad (11)$$

where s_i is the slope of $cell_i$, and k_i is a coefficient related to different land use types and surface roughness (m/s), which is different from the soil erodibility factor (K). In this study, the k_i value was determined according to Ferro and Porto (2000) and Fernandez, Wu, McCool, and Stockle (2003). In this study, the values of K were 2.62, 0.75, 2.13, 5.14 and 4.91 for farmland, forest, grassland, residential areas and water, respectively. To successfully calculate t_i, the minimum cell slope was set to a small value (e.g., 0.3% in this study). The basin-specific parameter β related to the morphological data of the watershed. Fu et al. (2004) found that the sediment yield was sensitive to the change of β, ranging from 0.5 to 2.0. Jain and Kothyari (2000) found that the sensitivity for sediment delivery ratio was different according to different watershed, and the sediment yield was sensitive to β when this value located in the range of 0.1–1.6. In this study, we found that the error was the least when the β was equal to 0.2. Therefore, in this study, β was set to 0.2. In this study, l_i was determined using ArcGIS and the Hydrological analysis module. In this study area, the range of sediment delivery ratio was 0.82–0.98, and the all average value was approaches to 0.9. This result was consistent with the finding of Jing (1999).

Therefore, the sediment yield of each grid cell was estimated as the following Eq. (12):

$$Y_i = SDR_i A_i a_i \quad (12)$$

where A_i is the soil erosion rate of each grid cell calculated by the RUSLE model and SDR_i is the *SDR* for $cell_i$.

The SEDD model was calibrated for the study area from 2000 to 2010. We selected the land use in 2000 and 2010 to calibrate the SEDD model, and land use data from 2000 and 2010 were used to calculate sediment yield from 2000 to 2005 and from 2006 to 2010, respectively. In this catchment, check dams are part of the conservation measures; 288 silt dams were built by 2010, and the controlled area was as high as 525.5 km^2, accounting for approximately 15% of the study area. Given that all of the check dams were filled with sediment, the sediment intercepted by all of the check dams would account for only 0.026% of all sediment yields in that year. Therefore, in this study, the impacts of check dams on sediment yield were ignored. After calibration, the SEDD model was used to calculate the sediment load based on the mean annual erosive rainfall data for land use scenarios (1990, 2000 and 2010) without consideration of the effects of check dams. SDR is shown in Fig. 2f.

4. Results

4.1. Changes of land use types in the basin

Since 1999, the implementation of the Grain for Green project was successful in improving the vegetation coverage in the study area. The changes in land use types at the three years are calculated in Table 1, and land use maps are shown in Fig. 3. The results showed that the dominant land use types were farmland and

Table 1
Land use changes from 1990 to 2010 in the catchment.

Land use type	1990		2000		2010	
	Area/km^2	%	Area /km^2	%	Area /km^2	%
Farmland	1594.75	46.79	1454.88	42.69	497.25	14.59
Grassland	1701.92	49.94	1847.14	54.20	2161.60	63.43
Forest	95.32	2.80	100.20	2.94	714.12	20.95
Residential area	12.14	0.36	2.83	0.08	17.76	0.52
Water bodies	3.87	0.11	3.07	0.09	17.26	0.51

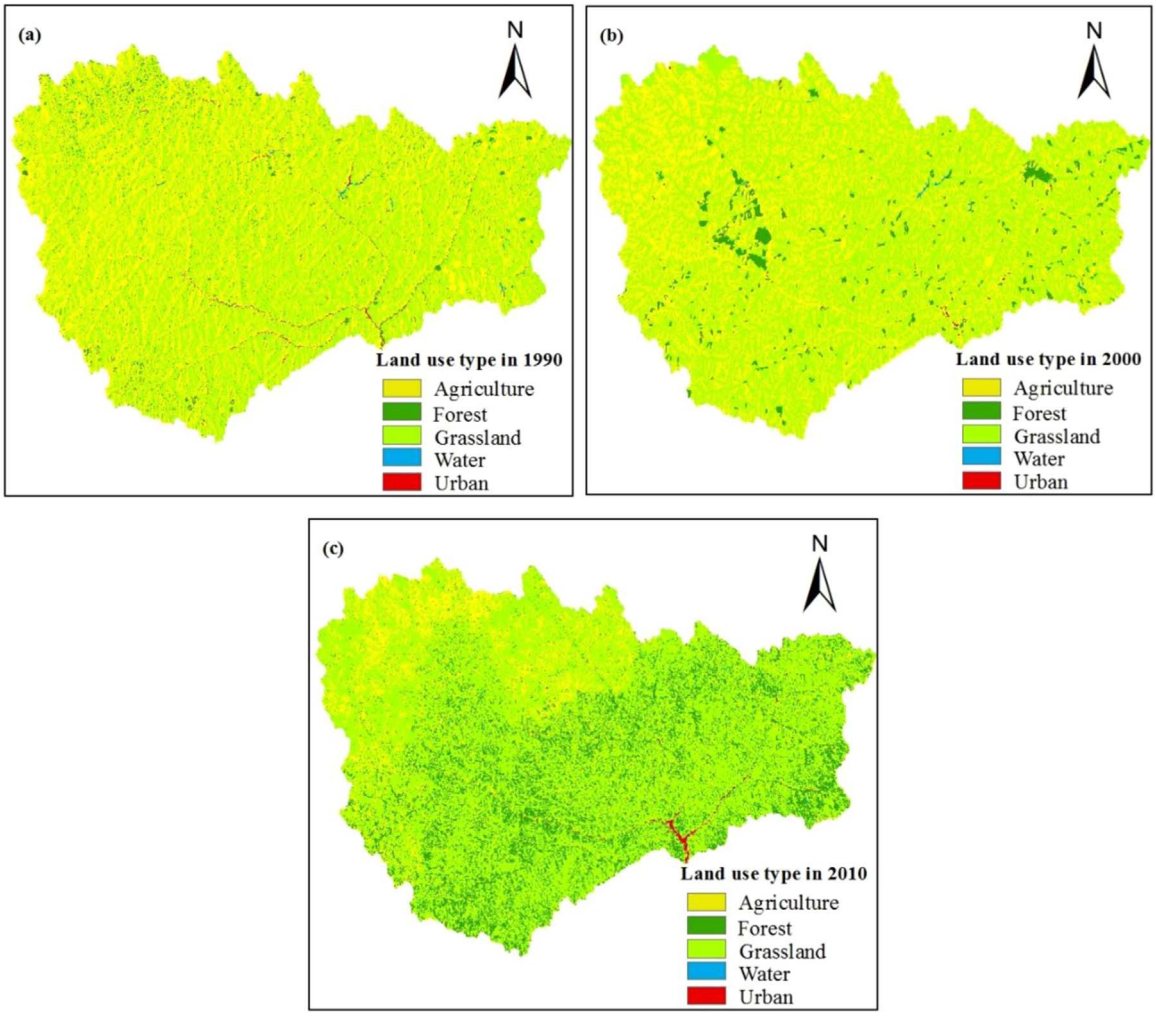

Fig. 3. Land use changes in the upper reaches of the Beiluo River basin in 1990, 2000 and 2010.

grassland, which accounted for 46.79% and 49.94% of study area in 1990, respectively. By 2000, farmland and grassland always dominated the region, but farmland gradually decreased by 4.1%, and grassland and forest increased by 4.26% and 0.14%, respectively. Until 2010, grassland and forest dominated the region. Compared with 2000, farmland decreased by 28.1%, whereas the grassland and forest rapidly increased by 9.23% and 18.01%, respectively. Generally, from 1990 to 2000, the farmland slowly decreased, whereas the grassland and forest slowly increased. It should be noted that residential area decreased from 1990 to 2000 probably due to the different data sources. However the increasing trend from 1990 to 2010 was correct and it may not impact the main content in this work. From 2000–2010, farmland rapidly decreased, whereas the grassland and forest rapidly increased. The trend was consistent with land cover changes under the background of Grain for Green project.

4.2. Model calibration and validation

Fig. 4 shows the results of the relationship between the measured and simulated sediment load at Wuqi station from 2000 to 2010 compared with the 1:1 line. The simulated results were satisfactory for the RUSLE, with good agreement between the simulated and measured sediment loads based on $R^2 > 0.8$ for the study period. However, we also found that the simulated results overestimated the sediment load in several years compared to the sediment load at the outlet of the basin. The range of simulated

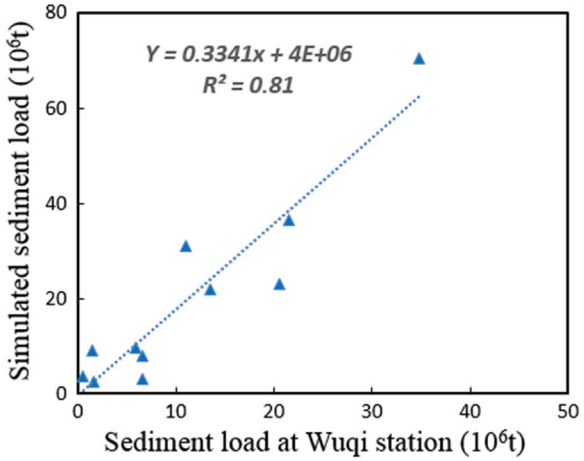

Fig. 4. Comparison of the measured and simulated sediment yield in the catchment.

results from 1.5×10^6 t in 2008–30.7×10^6 t in 2001 was consistent with the measured values at the Wuqi station from 0.57×10^6 t to 20.5×10^6 t. The simulated results tended to simulate the trends for the sediment load from 2000 to 2010, despite overestimating the sediment load. Therefore, the RUSLE model was used to estimate the soil erosion in 1990 compared to the measured value.

Please cite this article as: Yan, R., et al. *International Soil and Water Conservation Research* (2018), https://doi.org/10.1016/j.iswcr.2017.12.002

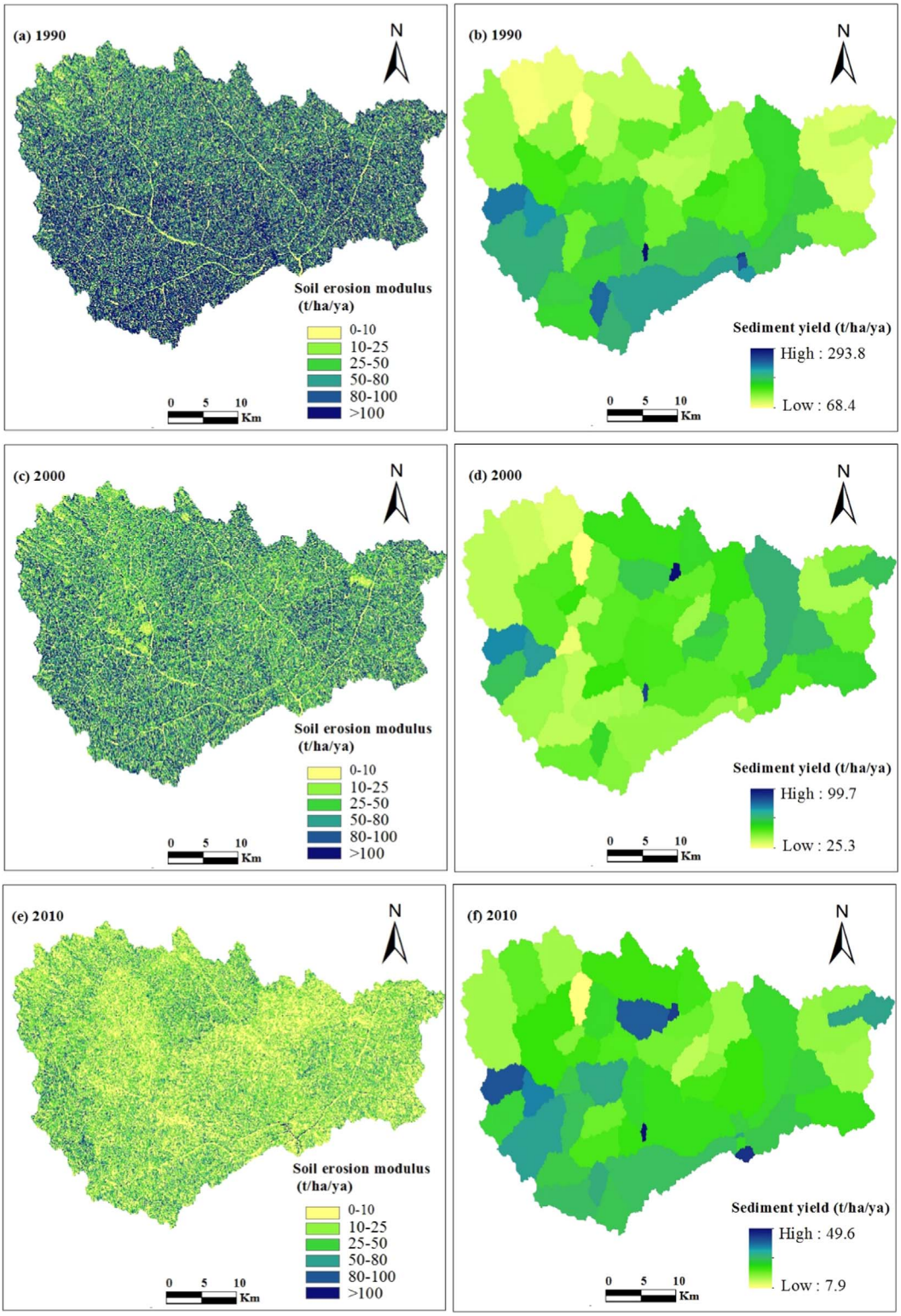

Fig. 5. Spatial distribution of soil erosion and sediment yield in 1990, 2000, 2010 in the study area.

4.3. Annual soil erosion estimation

The spatio-temporal distribution of soil erosion results and sediment yields of the basin in 1990, 2000 and 2010 are shown in Fig. 5. The research found that both the soil erosion and sediment yield presented a decreasing trend from 1990 to 2010, which may be attributed to the implementation of the projects, resulting in the improved vegetation coverage in the basin (see Table 2). Fig. 5 also shows that the total soil erosion amounts were 51.87×10^6 t, 22.05×10^6 t and 8.83×10^6 t for 1990, 2000 and 2010, respectively. The reason for the too high soil erosion intensity in 1990 may be that the precipitation in 1990 was higher than other years. The total sediment yield amounts were 48.03×10^6 t, 20.44×10^6 t and 8.16×10^6 t, respectively. The sediment yield decreased by 2.8 t/yr from 1990 to 2000, and from 2000 to 2010 the average value continued to decrease by 1.23 t/yr, which can be attributed

Please cite this article as: Yan, R., et al. *International Soil and Water Conservation Research* (2018), https://doi.org/10.1016/j.iswcr.2017.12.002

Table 2
Distribution of soil erosion intensity from 1990 to 2010 in the catchment.

Soil Erosion Grade	Range t/(km^2 · a)	1990		2000		2010	
		Area/km^2	%	Area /km^2	%	Area /km^2	%
I	< 1000	727.76	21.15	836.82	24.55	1483.06	43.52
II	1000–2500	203.68	5.90	374.98	11.00	760.47	22.31
III	2500–5000	305.58	9.28	586.35	17.21	703.44	20.64
IV	5000–8000	332.29	10.31	594.64	17.45	269.62	7.91
V	8000–15000	656.83	19.28	609.99	17.90	135.75	3.98
VI	> 15000	1181.85	33.68	405.23	11.89	55.66	1.63

to the decreasing farmland and increasing grassland and forest. A decrease of 57.4% in total sediment yield in 2000 was found compared to that in 1990. Similarly, in 2010, the sediment yield continued to reduce by 60.1% compared with that in 2000. Note that the average annual vegetation coverage in 1990, 2000 and 2010 in the basin was 15.86%, 19.20% and 35.50%, respectively, which showed a gradually increasing trend. The relationship between sediment yield and vegetation coverage was negative.

The range of sediment yield in each sub-basin decreased from 7184.76 to 24,323.06 t/(km^2 yr) in 1990, to 4176.18–7772.47 t/(km^2 yr) in 2000, and 1318.08–6833.10 t/(km^2 yr) in 2010. This demonstrated the benefits of soil and conservations implemented in the catchment.

According to the classification of soil erosion severity, it was classified into six grades. The research shows that the areas of soil erosion of grades I, II and III gradually increased, whereas the grades of IV, V and VI gradually decreased from 1990 to 2010 (Table 2). The total areas of I and II in study area accounted for were 27.05%, 35.55% and 65.83% in 1990, 2000 and 2010, respectively, and the areas of III were 9.28%, 17.21% and 20.64%, respectively. The area of IV gradually increased from 1990 to 2000, whereas it gradually decreased from 2000 to 2010. The reason may be that part of V and VI converted into IV, which lead to the increasing area of IV from 1990 to 2000. The diversity of the soil erosion and sediment yield spatial distribution gradually increased from 1990 to 2010; the reason may be that under the implementation of the forest projects in the study area, the vegetation coverage clearly improved, which changed the processes of runoff generation and convergence, and the pattern of soil loss in the study area (Yan et al., 2016). Previous research showed that with the increased vegetation coverage, the soil physical and chemical properties were improved, which changed the water cycle of region, increasing evapotranspiration and reducing surface runoff (Yan et al., 2016).

4.4. Effects of land use changes on soil erosion

In consideration of how to better control the soil loss in the future, the relationship between soil erosion and land use types were analyzed. The dominant land use types were farmland, grassland and forest in the catchment. The distribution of land use types corresponding to the soil erosion are shown in Table 3. The research found that the soil erosion modulus varied with land use types in a decreasing order from residential areas > farmland > grassland > forest in 1990, 2000 and 2010. The average soil erosion of the same land use in the three years gradually decreased, and the reason was expected to intrinsically related with land cover changes with which the total vegetation coverage in 1990 was lower than that in 2000 and 2010 in this area. From 2000–2010, the average soil erosion of forest clearly decreased, which may be a result from the Grain for Green project. Under the project, the forest was mainly artificial forest and dominated by sea-buckthorn and *Robinia pseudoacacia* with the highest coverage. Meanwhile, fish-scale pits were also constructed in the forest land. These measures lead to the least erosion modules for the forest. Grassland was the largest area in the basin to facilitate, including planted grassland under the implementation of projects and afforestation under the close hillsides. In the basin, grassland area was larger than the others, accounting for the total area, and the vegetation coverage was mostly moderate and low levels of vegetation. Therefore, the erosion modules and total sediment yield of grassland were larger than those of forest. We found that the soil erosion amount of grassland on average accounted for 52.57% of the total soil erosion amount in the three years, which was larger than the other land use types. Hence, the results show that with the higher soil erosion modulus of farmland and low coverage grassland, these areas are the primary areas of preventing soil erosion.

4.5. Effects of different slope gradients on soil erosion

The average soil erosion of different slope gradients was derived from the overlay analysis between the slope gradient map and the sediment yield map in 1990, 2000 and 2010. The results are shown in Table 4 and demonstrated that the average erosion intensity and total sediment yield gradually increased along with the increasing slope gradients. The average erosion intensity in the slope grades of 0–5°, 5–8° and 8–15° was smaller than the average erosion intensity of the basin. The reason may be that slope gradients below 20° belong to the gentle slope zone, and since the 1990s, these areas in Wuqi County experienced a big transformation under the prohibition of open grazing and abandoned cultivation for a large area of sloping land. By the end of 2007, Wuqi County had abandoned 12,000 ha of cropland and changed the others to terrace fields. The area in Wuqi County was the largest among all of the counties that abandoned cropland, approximately half of which was afforested (Yan et al., 2016). Therefore, in these moderate slope areas, the soil erosion intensity was smaller than the others. The soil erosion intensity in the slope grades of 15–25°, 25–35° and > 35° was larger than the average soil erosion intensity of the basin. The reason may be that the steeper the slope, the larger the runoff rate caused. These

Table 3
Soil erosion of different land use types from 1990 to 2010 in the catchment.

Land use type	1990		2000		2010	
	Average soil erosion t/(km^2 a)	Amount /10^5 t	Average soil erosion t/(km^2 a)	Amount /10^{5}t	Average soil erosion t/(km^2 a)	Amount /10^5 t
Farmland	19,920.33	159.09	9679.35	140.96	5810.72	28.89
Grassland	14,583.35	341.79	4138.84	76.77	2282.61	49.68
Forest	9945.66	13.98	1684.21	1.70	755.20	5.43
Residential area	19,944.46	2.43	15,986.95	0.39	20,220.97	3.61

Please cite this article as: Yan, R., et al. *International Soil and Water Conservation Research* (2018), https://doi.org/10.1016/j.iswcr.2017.12.002

Table 4
Soil erosion on different slope gradients from 1990 to 2010 in the catchment.

Slope gradient /°	Area /km^2	1990		2000		2010	
		Average soil erosion t/(km^2 a)	Amount /10^5 t	Average soil erosion t/(km^2 a)	Amount /10^5 t	Average soil erosion t/(km^2 a)	Amount /10^5 t
0–5	335.3	3654.58	12.23	1469.12	4.89	719.13	2.41
5–8	294.1	5853.81	17.37	2655.53	7.84	1212.18	3.6
8–15	1040.7	9780.65	102.34	4600.78	47.98	2002.53	20.95
15–25	1338.2	19,196.16	258.97	8145.82	109.69	3227.62	43.55
25–35	380	31,505.67	119.97	12,380.8	47.09	4387.66	16.71
> 35	20.2	39,147.46	7.83	15,201.57	3.04	5597.47	1.12

situations provided a topographic condition of intensive erosion. Meanwhile, the vegetation coverage was lower in the steep slope areas, in which the vegetation could hardly be provided growing conditions. The results also showed that the slope grade zone of above 25° should be the key area for implementing soil and water conservation measures in which intensive soil erosion still exists.

4.6. Effects of different slope aspects on soil erosion

The average soil erosion of different slope aspects was derived from the overlay analysis between slope aspect maps and soil erosion maps in 1990, 2000 and 2010. The results are shown in Table 5 and found that the soil erosion in a unit area in different slope aspects displayed a gradually increasing order of shady slopes, semi-shady slopes, semi-sunny slopes and sunny slopes, noting that the soil erosion in unit areas in sunny slopes and semi-sunny slopes was clearly greater than that in unit areas in shady slopes and semi-shady slopes, where the soil erosion was clearly smaller than the average annual soil erosion intensity in three years. The total soil erosion of both sunny slopes and semi-sunny slopes accounted for approximately 55.6% of the total soil erosion amount in the study area, which was larger than that in the shady slopes and semi-shady slopes. The total soil erosion amount in semi-sunny slopes was larger than in sunny slopes, and the reason was that for the total area, the area of semi-sunny slopes was larger than that of sunny slopes. From 1990–2010, the average soil erosion modulus also gradually decreased in the same slope aspects. In this basin, water was the most important factor for vegetation growth, and the amount of water determined the vegetation growth. In semi-arid areas, most plants suffer a longer period of sunshine in sunny slopes than in shady slopes, which results in a smaller soil water content, which is the main limiting factor to the plants. Yan et al. (2016) found that with the implementation of soil and water conservations, vegetation recovered more quickly in shady slopes than in sunny slopes in the upper reaches of the Beiluo River basin. Until 2014, the mean vegetation coverage in shady slopes and sunny slopes reached to 60–80% and 40–60%, respectively. The higher the vegetation coverage, the stronger the ability to retain water, which could reduce the amount of soil erosion. Therefore, the results show that the ecological construction should be continued on sunny slopes, which is also the key area for controlling the soil and water loss.

5. Conclusion

This study researched the land use changes from 1990 to 2000 and 2010 in the upper reaches of the Beiluo River basin. The result was presented by simulating the spatial distribution of soil erosion and sediment yield at a watershed scale with the combination of RUSLE and SEDD models. The distribution of soil erosion in different topographic factors was also analyzed. The conclusion can be summarized as follows:

From 1990–2000, farmland slowly decreased, whereas grassland and forest slowly increased. From 2000–2010, farmland rapidly decreased, whereas grassland and forest rapidly increased. In 2010, farmland area decreased by 68.8% and the grassland and forest increased by 27.0% and 18.15%, respectively. The RUSLE and SEDD models were calibrated using the observed sediment load data. There was good agreement between the measured and simulated values, indicating that the simulation results were satisfactory.

Scenario modeling indicated that the soil and water conservation measures were effective for sediment yield reduction in the study area. The amount of soil erosion and sediment yield gradually decreased from 1990 to 2010. The average soil erosion modulus decreased from 18,189.72 t/(km^2 yr) in 1990–7408.93 t/(km^2 yr) in 2000 and to 2857.76 t/(km^2 yr) in 2010. The average sediment yield modulus decreased from 14,093.31 t/(km^2 yr) in 1990–5997.65 t/(km^2 yr) in 2000 and to 2394.37 t/(km^2 yr) in 2010. The areas of soil erosion of grades I, II and III gradually increased, whereas the areas of soil erosion of grades IV, V and VI gradually decreased from 1990 to 2010. The remarkable reduction in sediment load measured at the Wuqi station is attributable to the implementation of soil and water conservation and subsequent Grain to Green program.

The results show that the soil erosion modulus varied with different land use types and decreased in the order of residential area > farmland > grassland > forest. The soil erosion amount of grassland in the total soil erosion amount was the largest compared to the other land use types because of its larger areas in the catchment. The results also found that the average soil erosion modulus gradually increased with the increase in slope gradient, and 76.08% of the total soil erosion was concentrated in the region with a gradient of more than 15°. The soil erosion modulus also

Table 5
Soil erosion of different slope aspects from 1990 to 2010 in the catchment.

Slope aspect	Area	1990		2000		2010	
	/km^2	Average soil erosion t/(km^2 a)	Amount /10^5 t	Average soil erosion t/(km^2 a)	Amount /10^5 t	Average soil erosion t/(km^2 a)	Amount /10^5 t
Sunny	803.12	18,607.75	127.91	7285.42	56.26	2790.85	22.91
Semi-sunny	891.66	16,138.29	174.46	6972.33	64.6	2756.02	24.45
Semi-shady	890.58	15,247.32	127.41	6320.27	54.35	2597	21.76
Shady	822.94	12,051.88	88.93	5455.83	45.32	2374.91	19.21

Please cite this article as: Yan, R., et al. *International Soil and Water Conservation Research* (2018), https://doi.org/10.1016/j.iswcr.2017.12.002

varied with slope aspect in the order of sunny slopes > half-sunny slopes > half-shady slopes > shady slopes. We also found that in the same slope and aspect zones, the average soil erosion modulus and erosion amount gradually decreased from 1990 to 2010. This research provides a useful reference for conservation measures and utilization in this area and offers a technical basis for using the RUSLE to estimate soil erosion on the Loess Plateau of China.

Acknowledgements

This study was supported by the National Natural Science Foundation of China (Grant nos. 41230852, 41440012 and 41101265), and Special-Funds of Scientific Research Programs of State Key Laboratory of Soil Erosion and Dryland Farming on the Loess Plateau (A314021403-C2).

References

Angulo-Martinez, M., & Begueria, S. (2009). Estimating rainfall erosivity from daily precipitation records: A comparison among methods using data from the Ebro Basin (NE Spain). *Journal of Hydrology*, *379*(*1*), 111–121.

Cai, C. F., Ding, S. W., & Shi, Z. H. (2000). Study of applying USLE and geographical information system IDRISI to predict soil erosion in small watershed. *Journal of Soil and Water Conservation*, *14*(*2*), 20–27.

Cheng, L. L., Zhao, W. W., Zhang, Y. H., & Xu, H. Y. (2009). Effect of spatial distribution of rainfall erosivity on soil loss at catchment scale. *Transactions of the Chinese Society of Agricultural Engineering*, *25*, 69–73.

Chen, L. D., Wang, J., Fu, B. J., & Qiu, Y. (2001). Land-use change in a small catchment of northern Loess Plateau, China. *Agriculture, Ecosystems and Environment*, *86*, 163–172.

Chen, N., Ma, T. Y., & Zhang, X. P. (2016). Response of soil erosion processes to land cover changes in the Loess Plateau of China: A case study on the Beiluo River basin. *Catena*, *136*, 118–127.

Fernandez, C., Wu, J. Q., McCool, D. K., & Stockle, C. O. (2003). Estimating water erosion and sediment yield with GIS, RUSLE, and SEDD. *Journal of Soil and Water Conservation*, *58*, 128–136.

Ferro, V., & Minacapilli, M. (1995). Sediment delivery processes at basin-scale. *Hydrological Science Journal*, *40*, 703–717.

Ferro, V., & Porto, P. (2000). Sediment delivery distributed (Sedd) model. *Journal of Hydrology Engineering*, *5*, 411–422.

Fitton, L., Saffouri, R., & Blair, R. (1995). Environmental and economic costs of soil erosion and conservation benefits. *Science*, *267*, 1117–1123.

Flanagan, D., & Laflen, J. (1997). The USDA water erosion prediction project (WEPP). *Eurasian Soil Science*, *30*, 524–530.

Fu, B. J. (1989). Soil erosion and its control in the Loess Plateau of China. *Soil Use and Management*, *5*, 76–81.

Fu, B. J., Meng, Q. H., Qiu, Y., Zhao, W. W., Zhang, Q. J., & Davidson, D. A. (2004). Effects of land use on soil erosion and nitrogen loss in the hilly area of the Loess Plateau, China. *Land Degradation & Development*, *15*, 87–96.

Fu, B. J., Zhao, W. W., & Chen, L. D. (2005). Assessment of soil erosion at large watershed scale using RUSLE and GIS: A case study in the Loess Plateau of China. *Land Degradation & Development*, *16*, 73–85.

Fu, B. J., Wang, Y. F., & Lu, Y. H. (2009). The effects of land-use combinations on soil erosion: A case study in the Loess Plateau of China. *Progress in Physical Geography*, *33*(*6*), 793–804.

Jain, M. K., & Kothyari, U. C. (2000). Estimation of soil erosion and sediment yield using GIS. *Hydrological Sciences Journal*, *45*(*5*), 771–786.

Jing, K. (1999). The regular of sediment transport in Jing River and Beiluo River Basin. *Yellow River*, *21*(*12*), 18–19.

Lal, R., & Bruce, J. (1999). The potential of world cropland soils to sequester C and mitigate the greenhouse effect. *Environmental Science & Policy*, *2*, 177–185.

Lee, S. (2004). Soil erosion assessment and its verification using the Universal Soil Loss Equation and Geographic Information System: A case study at Boun, Korea. *Environmental Geology*, *45*, 457–465.

Liu, B. Y., Nearing, M. A., & Risse, L. M. (1994). Slope gradient effects on soil loss for steep slopes. *Transactions of the ASAE*, *37*(*6*), 1835–1842.

Liu, B. Y., Nearing, M. A., Shi, P. J., & Jia, Z. W. (2000). Slope length effects on soil loss for steep slopes. *Soil Science Society of America Journal*, *64*, 1759–1763.

Liu, E. J., Zhang, X. P., Xie, M. L., Chen, N., Zhang, T. T., Guo, M. J., & Zhang, J. J. (2015). Hydrologic responses to vegetation restoration and their driving forces in a catchment in the Loess hilly-gully area: A case study in the upper reaches of Beiluo River. *Acta Ecologica Sinica*, *35*(*3*), 622–629.

Lu, F. F., Tenywa, M. M., Isabirye, M., Majaliwa, M. G., & Woomer, P. L. (2003). Prediction of soil erosion in a Lake Victoria basin catchment using GIS based Universal Soil loss mode. *Agricultural Systems*, *76*, 883–894.

McCool, D. K., Foster, G. R., Mutchler, C. K., & Meyer, L. D. (1989). Revised slope length factor for the universal soil loss equation. *Transactions of the Asae American Society of Agricultural Engineers*, *32*, 1571–1576.

Mitasova, H., Hofierka, J., Zlocha, M., & Iverson, L. R. (1996). Modeling topographic potential for erosion and deposition using GIS. *International Journal of Geographical Information Science*, *10*, 629–641.

Nearing, M. A. (2005). Modeling response of soil erosion and runoff to changes in precipitation and cover. *Catena*, *61*, 131–154.

Parysow, P., Wang, G. X., & Gertner, G. (2003). Spatial uncertainty analysis for mapping soil erodibility based on joint sequential simulation. *Catena*, *53*(*1*), 65–78.

Pimental, D., Harvey, C., & Resosudarmo, P. (1995). Environmental and economic costs of soil erosion and conservation benefits. *Science*, *267*, 1117–1123.

Qin, W., & Zhu, Q. K. (2009). Soil erosion assessment of small watershed in Loess Plateau based on GIS and RUSLE. *Transactions of the CSAE*, *25*(*8*), 157–165.

Renard, K. G., Foster, G. R., & Weesies, G. A. (1997). *Predicting soil erosion by water: A guide to conservation planning with the Revised Universal Soil Loss Equation (RUSLE)* (p. 703) Washington: USDA. Agriculture Handbook.

Ritsema, C. J. (2003). Introduction: Soil erosion and participatory land use planning on the Loess Plateau in China. *Catena*, *54*(*1*), 1–5.

Sun, W. Y., Shao, Q. Q., & Liu, J. Y. (2013). Soil erosion and its response to the changes of precipitation and vegetation cover on the Loess Plateau. *Journal of Geographical Sciences*, *23*, 1091–1106.

Sun, W. Y., Shao, Q. Q., & Liu, J. Y. (2014). Assessing the effects of land use and topography on soil erosion on the Loess Plateau in China. *Catena*, *121*, 151–163.

Wang, H. S., & Liu, G. B. (1999). Analysis on vegetation structures and their control on soil erosion. *Journal of Arid Land Resources and Environment*, *13*(*2*), 62–68.

Williams, J. R., Renard, K. G., & Dyke, P. T. (1983). EPIC-A new method for assessing erosion effect on soil productivity. *Journal of Soil and Water Conservation*, *38*(*5*), 381–383.

Wischmeier, W. H., Johnson, C. B., & Cross, B. V. (1971). A soil erodibility nomograph for farmland and construction sites. *Journal of Soil and Water Conservation*, *26*(*5*), 189–193.

Wischmeier, W. H., & Smith, D. D. (1978). Predicting rainfall erosion losses. USDA agriculture handbook. *US Department of Agriculture* (pp. 21–22), 21–22.

Xin, Z. B., Yu, X. X., Li, Q. Y., & Lu, X. X. (2011). Spatiotemporal variation in rainfall erosivity on the Chinese Loess Plateau during the period 1956–2008. *Regional Environment Change*, *11*(*1*), 149–159.

Yan, R., Zhang, X. P., Yan, S. J., & Zhao, W. H. (2016). Topographical distribution characteristics of vegetation restoration in the Beiluo River Basin from 1995 to 2014. *Journal of Northeastern University (Natural Science)*, *37*(*11*), 1599–1603.

Zhang, W. B., & Fu, J. S. (2003). Rainfall erosivity estimation under different rainfall amount. *Resources Science*, *25*(*1*), 36–42.

Zhang, Y., Liu, B. Y., Shi, P. J., & Jiang, Z. S. (2001). Crop cover factor estimating for soil loss prediction. *Acta Ecologica Sinica*, *21*, 1050–1056.

Zhao, G. J., Kondolf, G. M., Mu, X. M., & Han, M. W. (2017). Sediment yield reduction associated with land use changes and check dams in a catchment of the Loess Plateau, China. *Catena*, *148*, 126–137.

Please cite this article as: Yan, R., et al. *International Soil and Water Conservation Research* (2018), https://doi.org/10.1016/j.iswcr.2017.12.002